

Preliminary Design of the Hybrid Navigation System (HNS) for the CALLISTO RLV Demonstrator

René Schwarz^{1*†}, Marco Solari^{2†}, Bronislovas Razgus^{3†}, Michael Dumke^{4†}, Markus Markgraf^{5‡},
Matias Bestard Körner^{6†}, Dennis Pfau^{7§}, Martin Reigenborn^{8†}, Benjamin Braun^{9‡}, Jan Sommer^{10§}

[†] German Aerospace Center (DLR), Institute of Space Systems
Robert-Hooke-Str. 7, DE–28359 Bremen, Germany

[‡] German Aerospace Center (DLR), Space Operations and Astronaut Training
Oberpfaffenhofen, DE–82234 Weßling, Germany

[§] German Aerospace Center (DLR), Simulation and Software Technology
Lilienthalplatz 7, DE–38108 Braunschweig, Germany

* Corresponding author

Abstract

This paper focuses on the preliminary design of the Hybrid Navigation System (HNS) in development for the CALLISTO vehicle. The requirements and boundary conditions derived from the mission design are briefly introduced and their impact on the navigation design is discussed. Subsequently, the baseline architecture for the CALLISTO HNS including the design considerations for its sensor suite will be presented. The HNS features an approach that overcomes limitations of conventional navigation based on purely inertial solutions by fusion of measurements from different sensors. In order to satisfy the requested high accuracy in terms of estimation of vertical and lateral position as well as the flight altitude w. r. t. the landing pad, the sensor suite will comprise radar altimeters and a Differential GNSS (DGNSS) system along with ground-based reference stations. The paper concludes with a preliminary performance study of this HNS configuration through covariance analysis and an outlook on the further development of the system.

1. Introduction

In order to make access to space more affordable for both scientific and commercial activities, the French National Center for Space Studies (CNES), the German Aerospace Center (DLR), and the Japan Aerospace Exploration Agency (JAXA) joined in a trilateral agreement to develop and demonstrate the technologies that will be needed for future reusable launch vehicles. In the joint project Cooperative Action Leading to Launcher Innovation for Stage Tossback Operation (CALLISTO), a demonstrator for a reusable Vertical Takeoff, Vertical Landing (VTVL) rocket, acting as first stage, is developed and built. As long-term objective, this project aims at paving the way to develop a rocket that can be reused. The combined efforts of the three agencies will culminate in a demonstrator that will perform its first flights from the Guiana Space Center (CSG) in Kourou, French Guiana.

Several vertical landings of CALLISTO on a platform in the open sea off the coast of French Guiana are foreseen in the current mission design [1]. Such flights and landings pose challenging requirements on the development of a Guidance, Navigation and Control (GNC) system at large. This paper particularly focuses on the preliminary design of the Hybrid Navigation System (HNS), which is developed under the lead of the Department of GNC Systems of the DLR Institute of Space Systems for the CALLISTO vehicle. It is a standalone, robust, compact, hybrid system meant for integration into a distributed GNC system. Major contributions are coming from the Global Navigation Satellite System (GNSS) Technology and Navigation Group of the German Space Operations Center (GSOC) at DLR’s Facility for Space Operations and Astronaut Training with the design and development of the Differential GNSS (DGNSS) system

Revised paper as of July 1, 2019

¹E-Mail: rene.schwarz@dlr.de, ORCID: 0000-0002-8255-9451

²E-Mail: marco.solari@dlr.de

³E-Mail: bronislovas.razgus@dlr.de

⁴E-Mail: michael.dumke@dlr.de, ORCID: 0000-0002-5587-7884

⁵E-Mail: markus.markgraf@dlr.de

⁶E-Mail: matias.koerner@dlr.de

⁷E-Mail: dennis.pfau@dlr.de

⁸E-Mail: martin.reigenborn@dlr.de

⁹E-Mail: benjamin.braun@dlr.de, ORCID: 0000-0002-0193-6607

¹⁰E-Mail: jan.sommer@dlr.de

and from the On-Board Software Systems Group of the Department of Software for Space Systems and Interactive Visualization at DLR's Facility for Simulation and Software Technology with the design and development of the base software running on the On-Board Computers (OBC) of the HNS.

The development of the HNS technology for space transportation systems started already back in 2007 at DLR [2, 3, 4, 5] and has been successfully demonstrated in the frame of the SHarp Edge Flight EXperiment II (SHEFEX II) mission and its flight in June 2012 [6, 7, 8, 9]. The HNS features an approach that overcomes limitations of conventional navigation based on purely inertial solutions by fusion of measurements from different sensors. Traditionally, the navigation of space transportation systems is realized by sole use of inertial measurements and is, thus, subject to drift due to continuous numerical integration of small measurement errors of acceleration and angular velocity into progressively increasing estimation errors of velocity, position, and attitude. This way, the accuracy of the navigation solution rapidly deteriorates over time and mainly depends on the quality of the Inertial Measurement Unit (IMU). The advantage of those systems is that they do not rely on any external reference, which makes them immune to interferences, jamming, or spoofing. The drawback is that — even with highest grade IMUs — the achievable navigation performance reaches a very low accuracy within a few minutes after system initialization, which is still enough for placing payloads into the desired orbit with sufficient accuracy, but unacceptable when space transportation systems shall be returned back to Earth with pinpoint landing capability.

VTVL Reusable Launch Vehicles (RLV) like CALLISTO, thus, require more advanced navigation approaches such as hybrid navigation. The term *hybrid navigation* refers to the combination of high-frequency inertial measurements with (generally lower frequency) data of other sensors like GNSS receivers, radar and laser altimeters, Sun sensors, star trackers, etc. by means of data fusion. Those sensors provide absolute measurements of certain physical quantities (e. g., position, velocity, orientation with reference to other objects, etc.) and enable to periodically correct for estimation errors resulting from the previously described integration drift mechanism. This way, the navigation solution calculated by a HNS can be kept long-term stable. This approach also allows for lowering IMU performance requirements while still achieving a superior medium- and long-term navigation accuracy compared to purely inertial navigation systems. The specific sensor suite of a HNS depends on the particular requirements and boundary conditions of each mission. DLR is currently involved into two RLV missions in parallel: CALLISTO (VTVL demonstrator) and the Reusability Flight Experiment (ReFEX), which is a Vertical Takeoff, Horizontal Landing (VTHL) RLV demonstrator. For both missions, a HNS is being developed by DLR which serves as operational navigation system within the GNC loop. The core technology is shared across these developments, but the specifically chosen sensor suite deviates significantly between the two HNS due to major differences of the mission requirements.

This paper focuses on the specific design of the CALLISTO HNS. The requirements and boundary conditions derived from the mission design are briefly introduced and their impact on the navigation design is discussed in Section 2. Subsequently, Section 3 discusses the baseline architecture for the CALLISTO HNS including the design considerations for its sensor suite. In order to satisfy the requested high accuracy in terms of estimation of vertical and lateral position as well as the flight altitude w. r. t. the landing pad, the sensor suite will comprise radar altimeters and a DGNSS system along with ground-based reference stations. This DGNSS concept is discussed in more detail in Section 4. The paper concludes with a preliminary performance study of the HNS configuration through covariance analysis in Section 5 and an outlook on the further development of the system (Section 6).

2. Mission and Vehicle

2.1 Mission Description

The main objective pursued by CALLISTO is the collection of technical and economical data with reference to the development and operation of a reusable launcher first stage. For this purpose, the capability of flying, recovering, and reusing a vehicle under representative conditions of an operational system shall be demonstrated. This implies achieving to master the key technologies needed for future VTVL RLV, such as approach and landing systems, retro-propulsion, cryogenic propellant management during highly dynamic maneuvers, and GNC, among others, in a relevant environment. CALLISTO is designed to mimic a vehicle architecture similar to an operational launcher which is capable to fly several times. The components used must thus either be completely reusable or easily refurbishable.

The reusability of CALLISTO allows for an affordable incremental test approach with increasing flight envelope and complexity. It is foreseen to conduct at least ten flights with CALLISTO, beginning with very low energy hop flights up to full demo

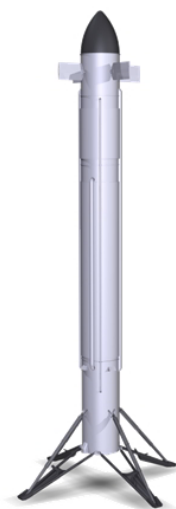


Figure 1: CAD rendering of CALLISTO.

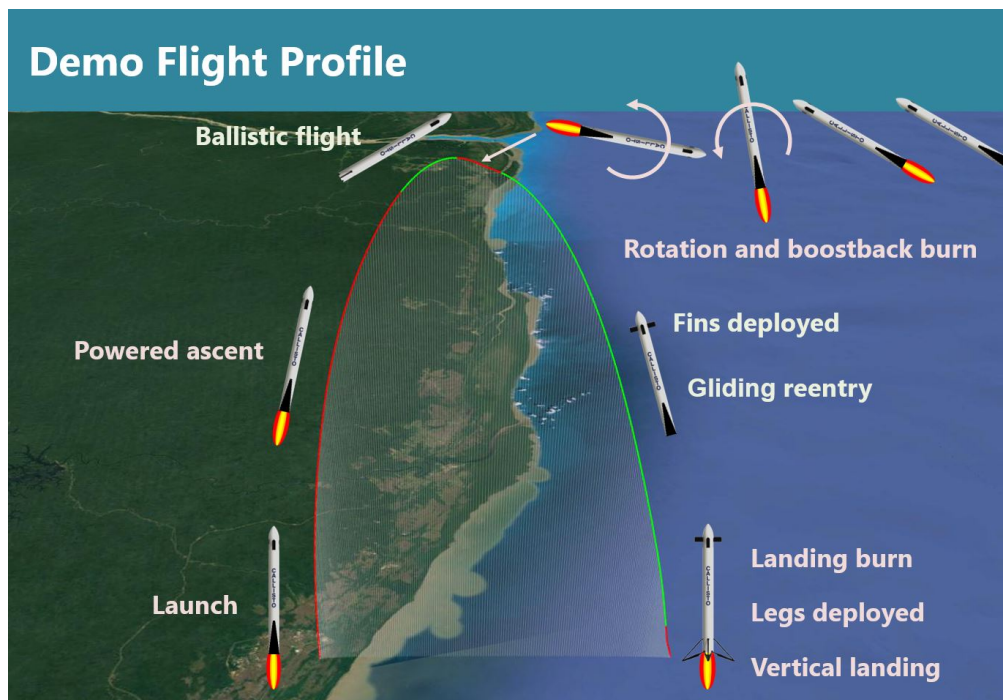


Figure 2: CALLISTO demo flight trajectory. Source: [10, supplemental conference material]

flight profiles with conditions expected to be representative and particularly critical for a reusable first stage (cf. Figure 2). All flights will be launched from CSG. The test flights will return back to landing pads on mainland, while the vehicle will land on a fixed platform in the open sea off the coast of French Guiana during the demo flights. An alternative landing option for the demo flights is a floating barge instead of a fixed platform; the trade-offs concerning this matter are not yet concluded. The project is currently in Phase B with the System Preliminary Design Review (PDR) scheduled later this year.

More details on the mission, its background and objectives, on other key technologies as well as on further related aspects can be found in [10, 11].

2.2 Vehicle Layout

The CALLISTO vehicle is 13.5 m high, has a diameter of 1.1 m, and its mass at lift-off is less than 4 t. The vehicle is composed of five primary sections (from the top to the bottom; cf. Figure 3): The *Fairing* provides an aerodynamic cover for the upper vehicle body, especially for the ascent phase. It houses a GNSS antenna integrated into the nose tip. The fairing is connected to the *Vehicle Equipment Bay (VEB)*, which accommodates the Flight Control System/Aerosurfaces (FCS/A), major parts of the vehicle avionics, including, among others, the OBC, the HNS, Flight Data Recorder (FDR), Data Acquisition Units (DAU), as well as the Flight Control System/Reaction Control System (FCS/R) including its tank in the upper part. The fairing and the VEB form the so-called Top Module. The Top Module is followed by the *Liquid Oxygen (LOx)* and *Liquid Hydrogen (LH2)* tank sections, which provide the propellants for the engine. In the lower part of the vehicle, an *Aft Bay* houses the rocket engine itself, the Flight Control System/Thrust Vectoring (FCS/V), additional avionics, and interfaces for the Approach and Landing System (ALS). The Aft Bay and the ALS form the Bottom Module.

The HNS is distributed to three of these sections: The HNS Box, the central part of the HNS, is accommodated within the VEB, while the GNSS antenna is integrated into the fairing and the radar altimeters are located outside on the Aft Bay.

2.3 Navigation Requirements and Boundary Conditions

The challenging design drivers for the HNS development are mainly the requested accuracies for the estimation of the vehicle's altitude above the landing pad as well as of the horizontal position, especially during the last part of the flight for approach and landing. From the Guidance and Control (G&C) studies conducted so far, a required estimation

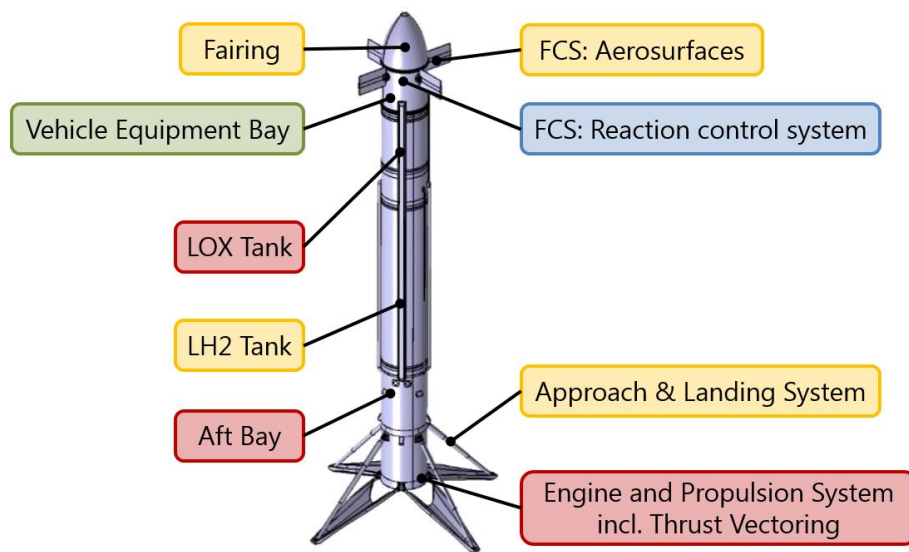


Figure 3: CALLISTO Vehicle Layout

accuracy for the altitude of 0.5 m and for the horizontal position of 1.0 m has been derived. In terms of attitude, an estimation accuracy of 0.3° for the yaw and pitch axes and 0.5° for the roll axis is called, respectively, while the attitude rate estimation accuracy for all axes shall be better than or equal to $0.1^\circ/\text{s}$. The velocity of the vehicle shall be estimated with at least 0.2 m/s accuracy. All aforementioned values are given at 99 % confidence and with the highest accuracy requested for each property from all flight phases.

Despite these key performances, additional major requirements and boundary conditions need to be addressed with the HNS design:

- The mass of the entire HNS, including all of its components and external sensors, shall be less than 13.2 kg.
- The navigation solution shall be delivered at 100 Hz.
- The HNS has to interface with the vehicle avionics via Ethernet using User Datagram Protocol (UDP) messages and a proprietary application-layer packetization standard.
- It has been chosen that the HNS will provide the authoritative time reference aboard the vehicle. It will distribute the time via the Precision Time Protocol (PTP) as defined by IEEE 1588-2002, whereas the HNS will serve as the PTP master within the avionics network.
- To have an additional localization mean of the vehicle — especially during the final flight phase — the HNS shall provide selected parts of the navigation solution at a lower rate as Immediate Visual Control (CVI) data to the Safety and Operational Coordination Quarter (SOCQ) to be used for flight safety purposes.

3. Architectural Design of the Hybrid Navigation System (HNS)

GNC systems can be implemented in very different forms, beginning with highly integrated systems combined together with all other functions of a spacecraft on a centralized OBC up to distributed systems with standalone elements for several functions. A highly integrated approach allows for optimizing mass, volume, and energy budgets, but usually requires a complete custom development for a particular mission, which often cannot be simply reused. On the other end, distributed systems with standalone elements allow for a certain partitioning of functions and mostly independent development. This way, the development and verification can be focused on the particular function more easily, with clear and defined interfaces to other functions. It also allows for a certain degree of modularity and exchangeability between different missions. Since CALLISTO is jointly developed by three agencies and with many industrial and research partners, it has been chosen to develop a distributed GNC system for the aforementioned reasons. A schematic of the simplified functional CALLISTO GNC architecture is provided with Figure 4.

The HNSs developed by DLR are standalone systems meant for integration into distributed GNC systems as described before. They implement the navigation function within the GNC loop and also include the necessary sensors and support electronics within their system boundaries. The heart of the HNS is a central electronics unit (called

HYBRID NAVIGATION SYSTEM (HNS) PRELIMINARY DESIGN FOR CALLISTO

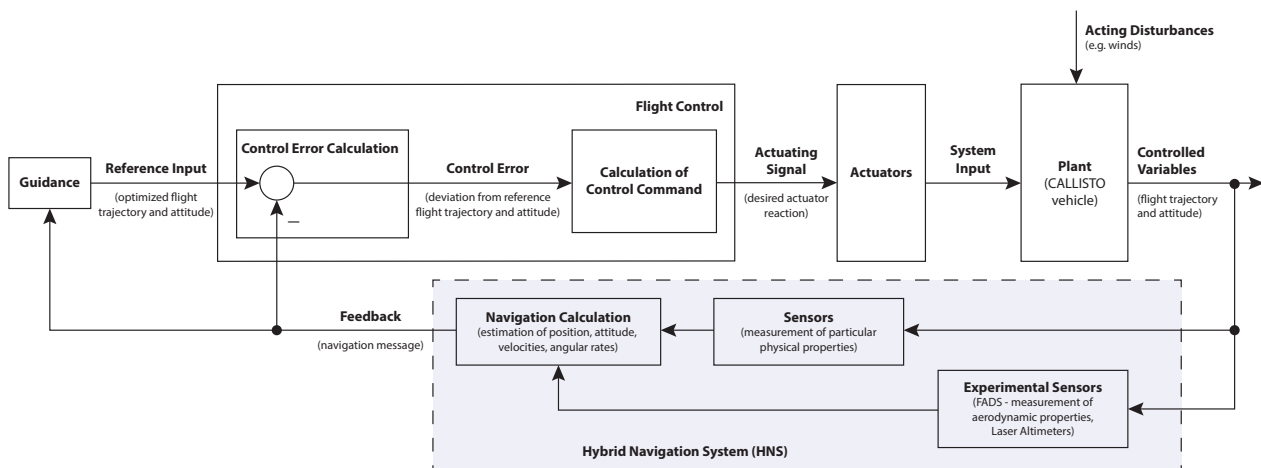


Figure 4: Simplified functional architecture of the GNC system to be developed for CALLISTO.

“HNS Box”), which houses a tetra-axial IMU consisting of four accelerometers and four gyroscopes, the navigation on-board computing and data handling components, the internal Power Distribution Unit (PDU), the GNSS receivers, and auxiliary electronics. It is designed internally in form of a hot-redundant fail-operational system architecture with Failure Detection, Isolation, and Recovery (FDIR) mechanisms both in terms of hardware and software to increase reliability and robustness against most outages or failures of individual sensors and components. In the specific case of CALLISTO, the HNS Box is connected to the vehicle avionics via an Ethernet network interface and communicates via UDP messages and a proprietary application-layer packetization protocol with the vehicle’s OBC, which is performing the G&C calculations, the Telemetry and Telecommand (TM/TC) gateway, and the FDR. External sensors are connected via serial communication links directly to the HNS Box, which supplies them with the required power at the same time. The HNS Box has therefore also the possibility to closely monitor the behavior of the external components and can power cycle or permanently turn them off in case of anomalies.

3.1 Fundamental Functions

Derived from the needs discussed in Section 2.3, the HNS will implement four fundamental functions:

- *Navigation as Part of the GNC Chain*

The apparent main function of the HNS is to provide a high-rate navigation solution, i. e., an estimation of the vehicle state (position, velocity, acceleration, attitude, rotation rate, flight altitude above landing pad, air density, Mach number, etc.) as feedback to the other elements of the GNC chain, and therefore to close the GNC loop.

- *Time Reference/Synchronization*

The HNS establishes the time reference for the entire CALLISTO vehicle and distributes the time via the standardized PTP over the avionics network. It acts as the PTP master, to which all connected avionics units can synchronize. Optionally, the HNS is capable of generating a dedicated electrical square wave signal accurately repeating once a second, called a Pulse Per Second (PPS), which can be used for phase and frequency synchronization of clocks within the vehicle. For all cases, the time base is directly derived from the GNSS measurements.

- *Navigation for Flight Safety Purposes*

To provide another source of information about the vehicle state for flight safety purposes, the HNS sends the estimated vehicle’s position and velocity via the TM/TC gateway to ground. These messages are provided at a lower rate than the navigation solution for G&C purposes and contain both the fused estimates based on all available sensors and the unprocessed information from the Position, Velocity, and Time (PVT) solution of the GNSS receivers. This is because the HNS itself is a technology demonstration, while the GNSS receiver technology is flight proven in many DLR missions and, thus, considered as very reliable. The receiver output is independent of the remaining HNS, despite of the powering via the internal PDU.

- *Navigation for Correlation of Experimental Data*

The navigation solution is used to correlate experimental data with navigation information. It is probably provided in a lower frequency than the navigation solution used for G&C.

3.2 Sensor Suite Considerations

A first assessment of the navigation performance necessary to fulfill the requirements from the flight control studies for the CALLISTO mission showed that the HNS sensor suite already defined for ReFEx was not sufficient to provide the required accuracy. Especially the requested accuracy for the estimation of the vertical and lateral position cannot be fulfilled out of the box by a single-frequency GNSS solution design without introduction of additional sensors.

Derived from CALLISTO project requirements, the design drivers for the HNS sensor suite can be divided into the following criteria:

- *Mass and Dimensions*: The sensor system overall mass and size shall be as low as possible.
- *Sensor Accommodation on Vehicle*: The geometry of the vehicle as well as the FCS/V limit the use of the lower side of the vehicle. Furthermore, the thermal environment near the engine and surrounding subsystems may interfere with the operation of the sensors.
- *Safety*: Active sensors may radiate electromagnetic beams or waves which will have to meet Electromagnetic Compatibility (EMC) requirements, not interfering with the communication system, or should not be harmful for humans, e. g., radar waves or lasers.
- *Procurement*: The sensor system shall consist of a Commercial Off-the-Shelf (COTS) system whenever possible to keep the costs and the risk down. International Traffic in Arms Regulations (ITAR)-controlled parts shall not be utilized.
- *Operational Environment*: The harsh environment of a rocket-driven vehicle requires a device with flight heritage, or at least high confidence on its proper functioning during the mission. Limitations of a given technology requires testing which is costly; e. g., if the influence of dust in the air is not known, better use dust-resistant technology. The CALLISTO flight is characterized by several cycles of re-ignition of the main engine. During the last phase of a flight from 2.5 km until touch down, the rocket engine is active, generating an exhaust plume that might interfere with an altimeter system during landing. Some technology needs additional Ground Support Equipment (GSE) that enhances the complexity and should thus be avoided, if possible.

The vertical position accuracy was identified as the design driver for a sensor suite selection and it was the starting point for a study on sensors able to enhance the vertical channel of the HNS. The evaluation was made on laser altimeters, radar altimeters, barometric altimeters, visual reference systems, GNSS receivers (including augmentation systems for satellite navigation), and beacon navigation.

Beacon systems are seen as adequate to improve the vertical accuracy of the navigation systems utilized in aeronautics, referred to as radio navigation: e. g., VHF Omni-Directional Range (VOR), Distance Measuring Equipment (DME), Non-Directional Beacon (NDB), or Instrument Landing System (ILS). However, the implied ground infrastructure is too complex to modify and adapt to the use case, and the regulatory effort to operate the system is very high, thus such systems were not further considered. Navigation satellite systems are a special kind of beacon systems that slowly replace the less accurate beacon systems listed before. GNSSs, and their augmentation, are later discussed in more detail for enhancing the horizontal accuracy of the navigation system.

Barometric systems were ruled out even though they are widely used in aeronautics. An aneroid barometer measures the static atmospheric pressure outside the vessel. The barometer has to be calibrated to the sea-level reference pressure, hence be adapted to local atmospheric conditions. The accuracy of the altimeter depends on the accuracy of the model used, the quality of the pressure measurement on the static port, and the accuracy on the sea-level measurement. It is robust, simple, and proved valuable from the upcoming of regulated air traffic until now within Unmanned Aerial Vehicles (UAV) (drones), but the drawbacks are the limited accuracy and the calibration to the environment on a rocket.

Visual navigation systems, like a *AprilTag*-based system, rely on a camera to identify a barcode, Quick Response (QR) code, or “tag” from a single image. These systems can be very robust and flexible, but drawbacks are the operational effort for a functional system, like camera calibration, GSE that needs additional calibration, changing lighting conditions, and significant interference of the engine plume.

Laser altimeters are sensors that measure the time between sending out a narrow laser impulse and receiving it back after being reflected by a surface. The Time of Flight (ToF) is the measure for the distance. Such sensors are a common way to measure distances with high accuracy, with high sample rates, and good repeatability. Nevertheless, the high sensitivity to dust, vapor, and the engine plume diminishes the advantages. Additionally, the correlation of the measurement of the ToF and the true height above ground is dependent on the attitude estimation accuracy of the vehicle, which has to be taken into account.

HYBRID NAVIGATION SYSTEM (HNS) PRELIMINARY DESIGN FOR CALLISTO

Finally, for the CALLISTO vehicle, *radar altimeters* have been identified as the most feasible solution to enhance the vertical accuracy of the HNS. Radar altimeters are also ToF sensors with electromagnetic carrier waves of frequencies in the range of 2 – 100 GHz. Typically, two antennas are necessary, separated for transmitting and receiving. The antennas can either be integrated within a common housing for antennas and electronics or separated from the electronics. Radar altimeters are common instruments within aeronautics used to measure the distance to the ground; they are also commonly used as highly reliable sensors for automatically landing aircraft. SpaceX uses a radar altimeter for the Falcon 9's first stage with 4.3 GHz [12] and also the Apollo lander used a radar altimeter [13]. COTS devices have generally a worse accuracy compared to laser altimeters but do not require to back-calculate the slanted range to the altitude above ground.

From all the investigated sensors, only the radar altimeter technology is considered to fulfill the CALLISTO requirements given the aforementioned criterions. Furthermore, the radar altimeter is expected to be resistant against the plume/exhaust and dust interactions. Disadvantages like the accommodation on the vehicle, and the limited accuracy are probably much easier to overcome than to prove another technology ready for a rocket engine propelled vehicle like CALLISTO. The selected baseline is thus the inclusion of at least one radar altimeter with integrated antennas to be accommodated on the Aft Bay.

The use of *GNSS augmentation systems* for altitude determination has been considered, but the achievable accuracy, reliability, and robustness have been evaluated as unsuitable for the vertical navigation solution. But the second major requirement for the navigation system, the horizontal accuracy, which a stand-alone GNSS receiver is not able to fulfill, is seen as a use case for an enhanced GNSS receiver system.

A simple DGNSS concept for CALLISTO consists of a GNSS receiver along with a suitable antenna aboard the rocket, a reference GNSS receiver and antenna on ground near the landing site, and a telemetry uplink for real-time correction data. The following technologies have been taken into account to increase the accuracy of horizontal/vertical position/velocity:

- *Multi-Constellation GNSS* improves the Position Dilution of Precision (PDOP) due to a larger number of satellites in view and more modern satellites with small satellite clock errors (Global Positioning System (GPS)-IIF, GPS-III A, Galileo).
- *Multi-Frequency GNSS* enables correction for ionospheric delay and increases accuracy due to enhanced ranging codes on new signals (GPS L1/L5, Galileo E1/E5).
- *DGNSS* enables instantaneous correction (via data uplink) for ionospheric delay, satellite orbit and clock errors, and ionosphere monitoring before launch (scintillations).
- A *Satellite-Based Augmentation System (SBAS)* enables partial reduction of ionospheric delay, satellite orbit and clock errors. French Guiana, however, is outside of the service area of the Wide Area Augmentation System (WAAS). Commercial services with satellite-based correction data broadcast enable partial reduction of ionospheric delay, satellite orbit and clock errors (e. g., OmniStar Virtual Base Station (VBS)). This creates a dependency on an external service whose availability is not guaranteed. Pseudorange (PR)-based DGNSS correction services may be discontinued in future. Special multi-frequency antennas are required.

The ground infrastructure for a DGNSS system increases the complexity of the CALLISTO system but it is seen as the sole solution to achieve the required navigation performance. Having said this, a combination of a DGNSS with a multi-constellation, multi-frequency GNSS concept has been chosen as baseline. On ground, DGNSS reference station(s) will provide corrections for PR and Pseudorange Rate (PRR) measurements for the DGNSS Subsystem (DGS) in Radio Technical Commission for Maritime Services (RTCM) format. If feasible and required, the reference station(s) can also generate data for Real-Time Kinematic (RTK) navigation. The reference station(s) are used for monitoring of jamming, spoofing, scintillation, and ionosphere. Section 3.3.1 introduces the DGS as a part of the HNS including the ground infrastructure and Section 4 shows the expected performance of this system for a CALLISTO flight.

3.3 Baseline Design

Figure 5 provides an overview about the HNS and its components. The main component is the HNS Box, which is a compact, self-contained compartment accommodating the inertial sensors, On-Board Computing and Data Handling (OBCDH) system, PDU, and auxiliary electronics. In terms of sensors, the HNS is equipped with an in-house built IMU, two GNSS receivers, and two radar altimeters. In addition to that, the HNS uses a ground-based DGNSS system (cf. Section 4) to increase the accuracy and robustness of the GNSS system. The ground segment includes DGNSS reference stations, an Attitude and Heading Reference System (AHRS), radar reflectors, and other infrastructure elements.

R. SCHWARZ, M. SOLARI, B. RAZGUS *et al.*

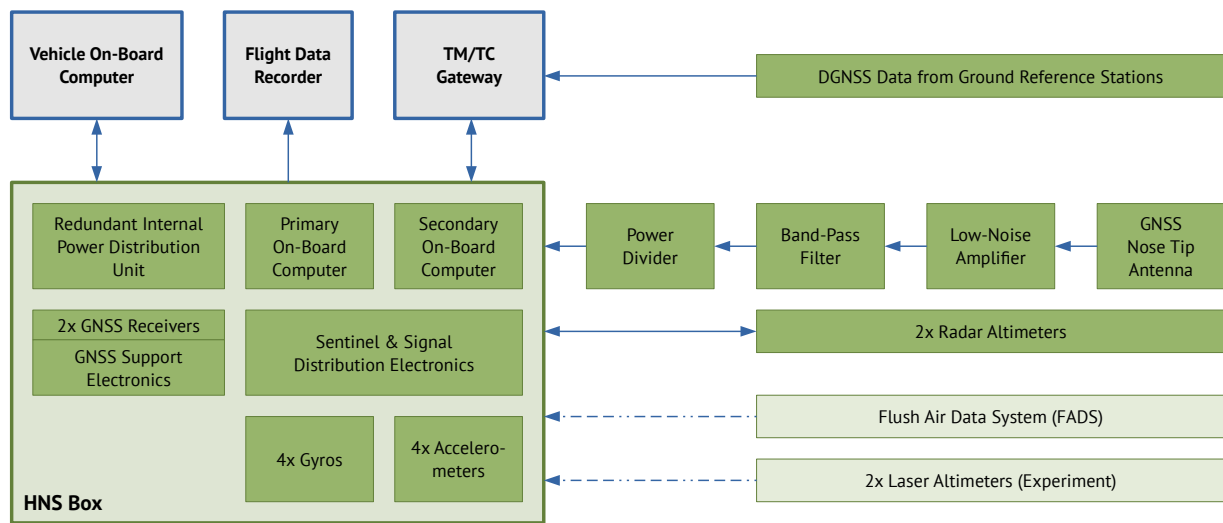


Figure 5: Overview of functional groups and components of the HNS. The connections between the components represent the data flow without further distinction between signal types.

Furthermore, including a Flush Air Data System (FADS) is proposed, but the necessity of air data measurements for G&C purposes is not yet confirmed.

The HNS Box is integrated into the VEB, while the GNSS antenna is located on the nose tip and the radar altimeters are to be accommodated on the Aft Bay.

3.3.1 Differential GNSS Subsystem (DGS)

The CALLISTO DGS is an integral part of the HNS that provides a major source of navigation information for real-time guidance and control. Beyond that it provides relevant data for post-flight trajectory analysis and range safety. Within the HNS, GNSS provides the primary source for absolute position information but also contributes relative position information with respect to the landing side. GNSS tracking will cover all flight phases from launch to landing, which poses special requirements on the GNSS receiver in terms of tracking under high signal dynamics and the environmental conditions.

The DGS is based on a hot-redundant pair of GNSS receivers (Figure 6) offering dual-frequency GPS and Galileo tracking on two frequencies (L1/L2 and E1/E5a). In view of engineering budgets (mass, power, form factor, etc.), a tight project schedule, and cost considerations, COTS receivers will be used that offer a high maturity as well as adequate robustness. Based on flight heritage from the earlier use on an Ariane 5 vehicle [14], Septentrio AsteRx-m2 receivers have been selected as primary candidates for the CALLISTO mission and are presently undergoing further testing and qualification.

The GNSS receivers will be jointly connected to an active antenna via a power splitter. The antenna itself will be integrated in the nose cone of the CALLISTO vehicle to provide hemispherical coverage. It is based on a NovAtel pinwheel antenna element supporting survey-grade GNSS measurements across the L1/E1, L2, and L5/E5a frequency band. The pinwheel antenna design [15] allows operation of the antenna without a dedicated ground plane and offers a high level of multipath suppression. A prototype nose cone with the integrated antenna element and low noise amplifier as shown in Figure 6 is currently undergoing testing and calibration of gain and phase patterns to qualify the design for the CALLISTO mission.

Aside from the on-board components, the DGS also comprises at least one ground-based reference station near the landing site (Figure 7). This reference station will collect GPS and Galileo observations that will be sent to CALLISTO via a radio-frequency Telecommand (TC) uplink. This enables a differential correction of the on-board observations to achieve enhanced accuracy and meet the demanding horizontal positioning knowledge required during the landing phase. Depending on the specific choice of landing site (land, fixed platform, moving platform), a permanently installed GNSS monitoring station, a temporary but static reference station, or a small network of receivers for position and orientation determination of a moving barge can be foreseen.

HYBRID NAVIGATION SYSTEM (HNS) PRELIMINARY DESIGN FOR CALLISTO

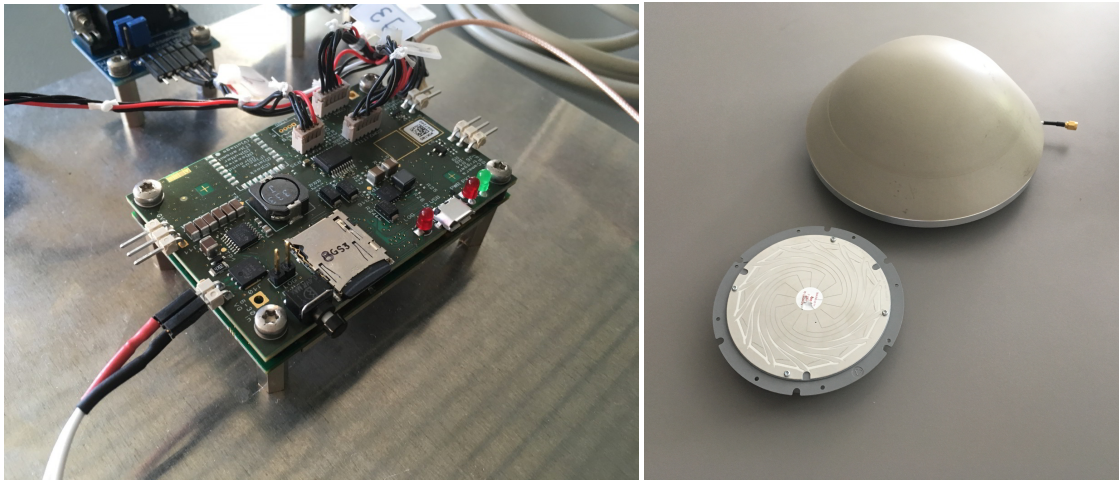


Figure 6: Core components of the DGNSS subsystem of CALLISTO: AsteRx-m2 multi-GNSS receiver including UAS extension board (left) and the nose cone antenna (right).

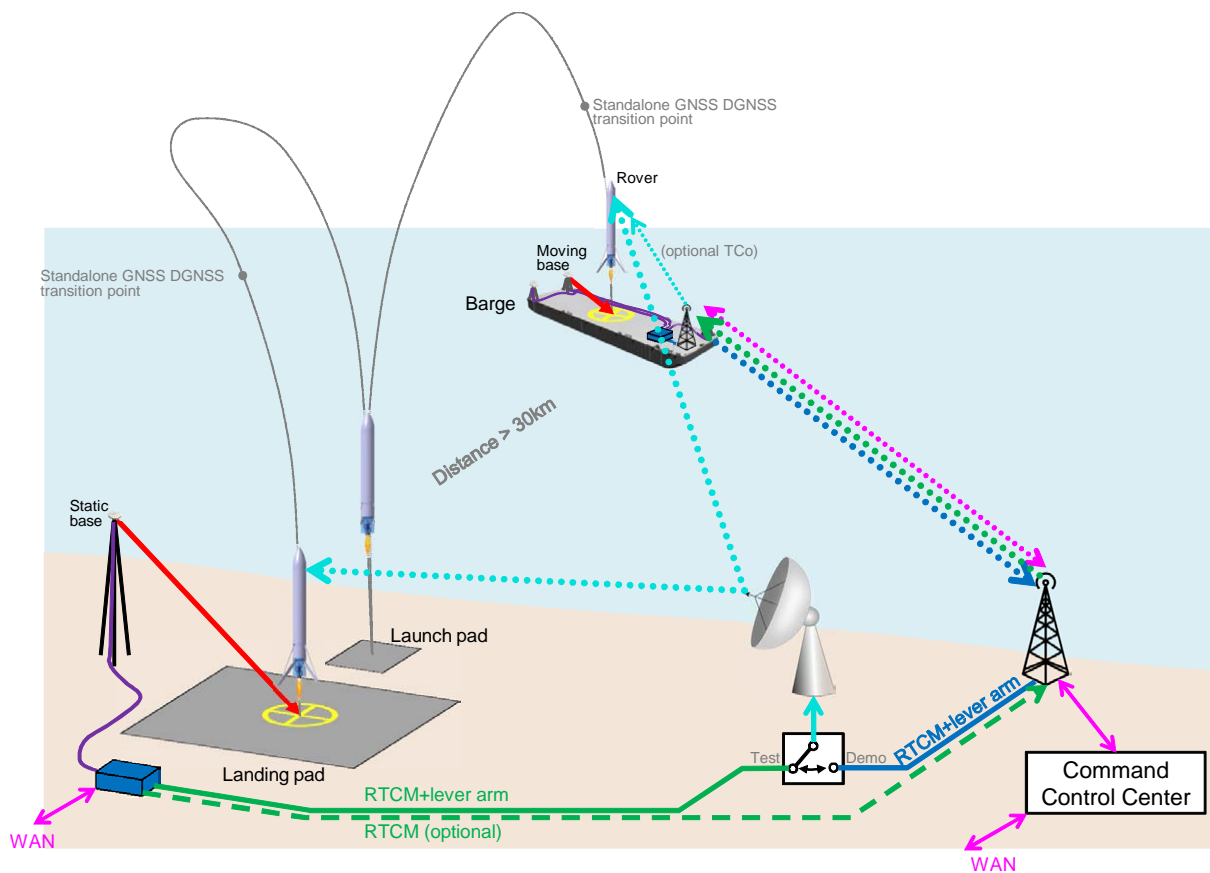


Figure 7: System architecture for absolute and DGNSS navigation during all flight phases of the CALLISTO vehicle.

3.3.2 Radar Altimeters

Previous analyses resulted in the selection of radar altimeters as the only satisfying solution for direct and high-accuracy measurements of the vehicle's flight altitude relative to the landing pad. As a side effect, radar altimeters are also capable of giving a direct measurement of the vehicle's approach velocity relative to the landing pad. However, there is no COTS radar altimeter solution available on the market which directly fulfills all requirements and constraints set by the mission. It is currently investigated whether and how existing radar sensors or technologies can be adapted for the CALLISTO HNS. Main challenges taken to be into account are

- the desired measurement principle,
- the unknown interaction of the signals with the engine plume, and
- the operational environment conditions arising from the accommodation.

Initially, a very simple measurement method similar to radar altimeters used for aircraft and UAVs was foreseen. In principle, such radar altimeters measure the distance between the aircraft and the terrain directly beneath it by sending out radio waves and measuring the time it takes to receive these signals back due to reflection on the ground (called Time of Flight (ToF)). Using the ToF measurement and the known speed of electromagnetic waves in air, the distance to ground can be calculated. In general, the ToF measurement is based on the first reflection received back, i. e., the nearest object within the spherical propagation direction whose radar cross section is large enough to be detected. This measurement principle would work for CALLISTO if the radar altimeter measurements would be needed only during a flight phase where the vehicle is already directly located above the landing pad, where the maximum tilt angle of the vehicle is smaller than the half beam angle of the antenna, and where no objects within the signal sphere tangent to the landing pad surface higher than the landing pad itself are present (cf. Figure 8 (left) for a visualization).

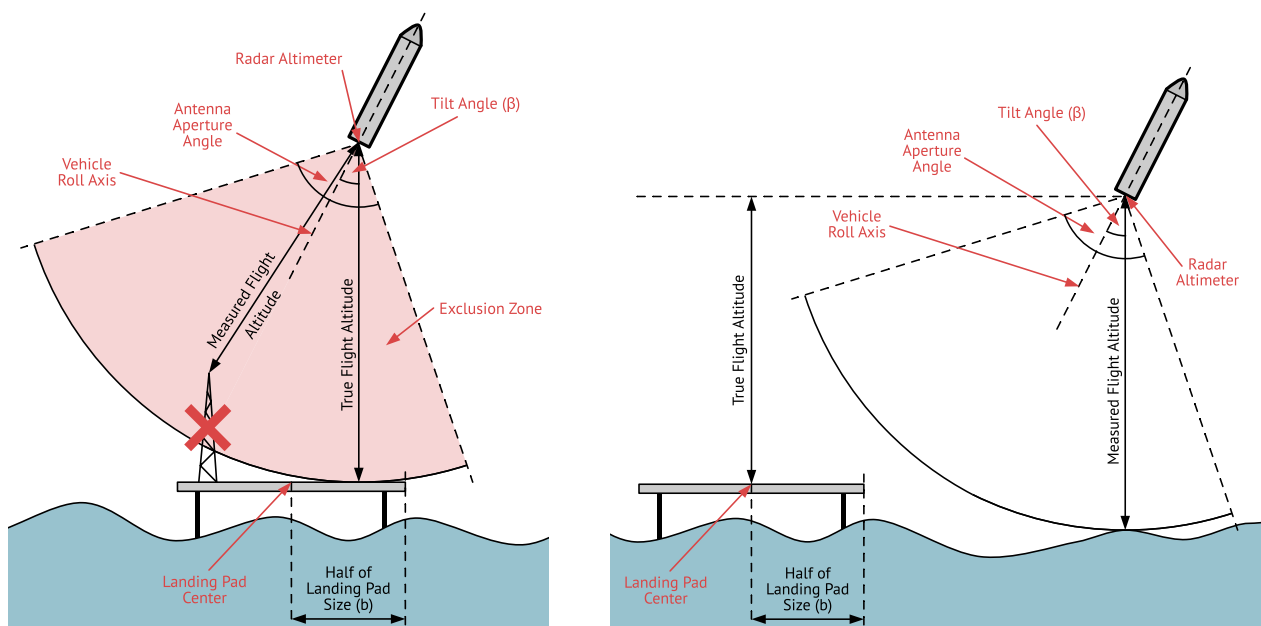


Figure 8: Schematic drawing of the simple radar altimeter measurement principle based on the nearest detectable object. Left picture: Case in which the vehicle is directly above landing pad. The red circular segment is the exclusion zone for the given true flight altitude, where no other objects must be present. Right picture: Vehicle with horizontal displacement to landing pad — nearest detectable is the water, not the landing platform.

In the course of the further studies it turned out that the radar altimeter measurements are already needed at a point in time when the vehicle is not yet located directly above the landing pad, but with a horizontal distance of some hundred meters. In this situation, the altitude above the terrain beneath the vehicle instead of the altitude above the landing pad would be measured (cf. right side of Figure 8). Additionally, keeping the required area clear of any higher objects turned out to be challenging. It was then decided to discard this simple measurement principle in favor of a concept which relies on identification of the landing pad center in the radar signals.

In this more complex measurement scenario, radar reflectors are placed in the landing pad center and around it, which can be identified in the received radar signals by specialized detection algorithms. The antenna aperture angle is chosen large enough to have the entire landing pad in the antenna Field of View (FoV), taking the maximum horizontal distance to the landing pad center and the maximum tilt angle of the vehicle into account. This way, also objects higher

HYBRID NAVIGATION SYSTEM (HNS) PRELIMINARY DESIGN FOR CALLISTO

than the landing pad itself (like the ground installations needed for DGNSS operation) are possible, given that they do not obstruct the view to the radar reflectors. A schematic drawing of this measurement principle is depicted in Figure 9.

Independent of the measurement principle, there is currently no experience with operating radar altimeters in the proximity of or even through the LH2/LOx engine exhaust plume. The engine exhaust plume could interfere with the radar measurements, potentially falsifying them or rendering valid measurements even impossible. A test campaign to collect experimental data of this interaction, if any, during an upcoming engine static firing test with radar altimeter prototypes is currently planned.

Another point to be addressed for the radar altimeters are the operational environmental conditions. As the altimeters will be operated close to the engine exhaust plume, they will be subject to very high temperatures, vibrations, and shocks. A protection and qualification concept still needs to be derived, as available radar sensors are usually not operated in such environments.

3.3.3 Inertial Measurement Unit

The proper functioning of the IMU is vital for the navigation system as the high-rate measurements of angular velocities and linear accelerations, integrated to generate a position, velocity, and attitude solution, ensure the continuity of the navigation output. This continuity is fundamental since possible gaps in the measuring of the high dynamics experienced by the CALLISTO vehicle could cause large losses in navigation solution accuracy which in turn could lead to unrecoverable flight states. The IMU is designed as tetra-axial configuration of four COTS gyroscopes and four COTS analog accelerometers with an in-house developed Front-End Electronics (FEE). This design allows a partly redundant linear acceleration and angular velocity measurement scheme, thus offering an over-determined measurement system for the three spatial axes. In the event of failure of one sensor, the remaining three sensors will still cover all three spatial axis. All components are mounted onto a self-developed mechanical structure.

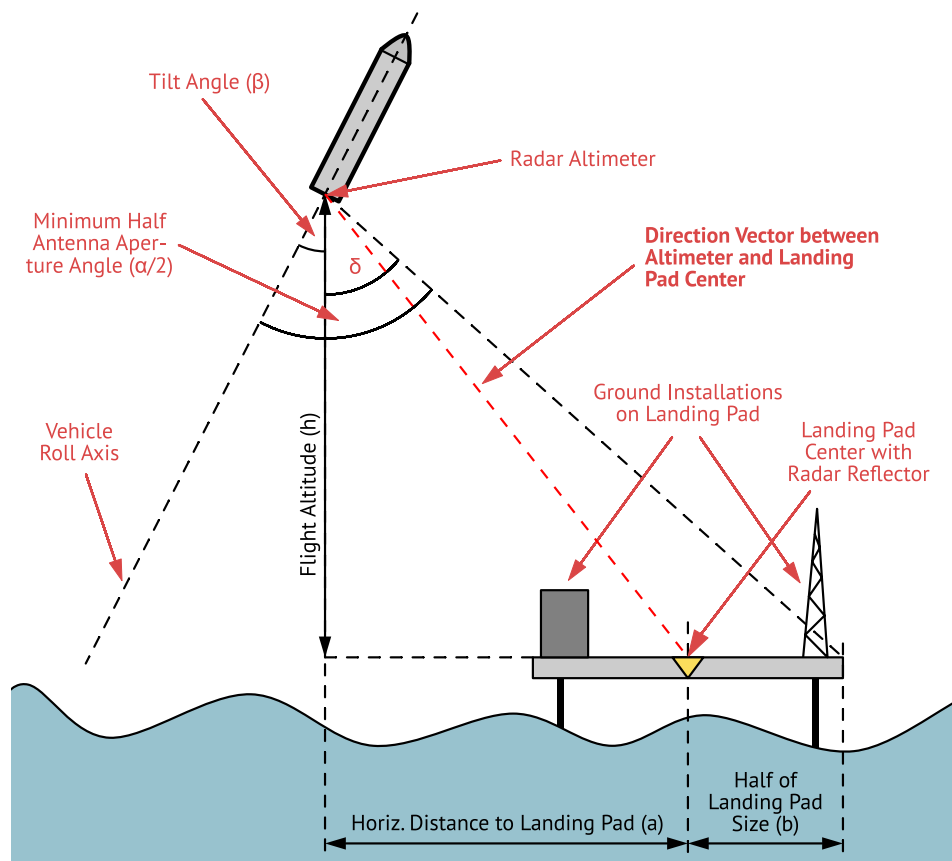


Figure 9: Schematic drawing of the radar altimeter measurement principle.

3.3.4 On-Board Computing & Data Handling

In order to enable the HNS to perform all its functions, a highly reliable, fault-tolerant OBCDH architecture with the necessary infrastructure components (e. g., a fully redundant PDU) incorporating a FDIR scheme is being developed. Its key characteristic is an augmented, double modular hot-redundancy scheme of two OBC nodes. The OBCs are stackable COTS single-board computers with Intel Atom Quad-Core Central Processing Units (CPU) in the standardized PC/104-Express format. The OBC stacks are extended with custom interface extension boards based on a Xilinx Spartan-6 Field-Programmable Gate Array (FPGA), providing a large amount of RS-422/485 serial communication links, General-Purpose Input/Outputs (GPIO), and Ethernet ports. Each OBC stack will be supplied by one in-house developed power supply board.

The OBCs are operated in a hot redundancy scheme, i. e., each OBC receives the data of all components and performs all calculations with the same on-board software. However, only one OBC is the *currently active OBC* whose outputs (commands) will be routed to the respective components within the HNS or to the outside world (i. e., the navigation solution, telemetry, etc.). All outputs of the other OBC (referred to as *standby OBC*) are suppressed by an electronic circuitry. In case of failure of the currently active OBC, the system can switch the roles of both OBCs, so that the output of the previous standby OBC will be routed. After switching the roles, the failing OBC will be power cycled and tested. There are various failure detection mechanisms in place in order to ensure a proper and timely role switch in case of failures.

The OBCDH systems closely interact with the PDU, which is controlled by the OBCs and delivers valuable monitoring data back. This way, it is also possible for the OBC to detect power anomalies and switch certain devices on or off to safeguard or recover the system operation. The PDU also plays a vital role for initialization of the HNS as it ensures a sequential and proper activation of all components, especially the OBCs.

3.3.5 Power Distribution

The PDU is the internal power supply for the CALLISTO HNS and is located within the HNS Box. It monitors and controls the supplied power for all devices belonging to the HNS. Since it is a 1-fault-tolerance power supply, a redundancy concept for its critical parts has been implemented [16, 17, 18]. The PDU Monitor (PDU-M) monitors currents, voltages, and temperatures within the HNS and transmits this information to the PDU Controller (PDU-C) to control each power channel output [19]. As an additional feature, all power channel outputs have an overvoltage protection.

Currently, the PDU has been configured with six power channels and 27 electronic power switches. Electromagnetic Interference (EMI) filters, resettable electronic fuses, electronic switches, Direct Current-to-Direct Current (DC/DC) converters, and O-Ring (OR) diodes are the main components of the PDU. EMI filters prevent the DC/DC converters' high-frequency currents to flow back to the vehicle power supply. Electronic resettable fuses protect each power switch against overcurrent. In case of an overcurrent condition, the fuses can be resetted by switching off and on the corresponding electronic switch. Primary switches control the DC/DC converters and secondary switches control the HNS devices supplied power, respectively. The DC/DC converters reduce the power bus voltage level coming from the vehicle power supply to the required ones. OR diodes isolate the DC/DC converter outputs to achieve a redundant output connection [20]. Figure 10 shows the basic PDU block diagram.

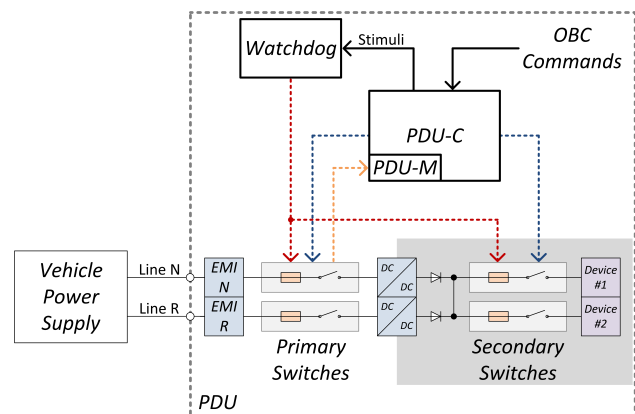


Figure 10: PDU Block Diagram

The redundant PDU concept enables the HNS devices to receive power from their redundant supply lines during an electronic switch failure. In addition, the PDU detects errors in the PDU-C through its watchdog circuitry when no or wrong stimuli signals are produced. The fail-safe mode procedure takes place when the PDU-C fails and activates all power channels outputs in consequence. Therefore, all HNS devices are powered. If the fail-safe mode is initiated, the electronic switches cannot be controlled anymore. However, since at this stage all HNS devices are switched on, the overall system operation is not affected [5].

3.3.6 Base Software

Part of the successful operation of the CALLISTO HNS is a reliable navigation software stack, meeting all requirements. The base software represents the lower and middle part of this software stack, which is running on both OBCs within the HNS. It contains the operating system, drivers, and middleware. A specialty of CALLISTO is that the vehicle OBC provided by DLR is almost identical to the OBCs used within the HNS, with the same COTS x86 multicore processor and similar interface devices. It allows to reuse large parts of the base software for all three OBCs.

The final navigation software stack will contain complex algorithms that need to be calculated in a certain time. It is expected that the computational workload needs to be distributed over multiple cores to meet the requirements. Therefore, Real-Time Operating System for Multiprocessor Systems (RTEMS) [21] was chosen as the real-time operating system. It provides full support for Symmetric Multiprocessing [22]. RTEMS can also look back on a long legacy in the space industry and was used by the DLR for its Compact Satellite mission “Euglena and Combined Regenerative Organic-Food Production in Space (Eu:CROPIS)” [23].

All subsystems of the launcher, including the HNS and the vehicle OBC, communicate with each other via Ethernet. RTEMS already provides a fully featured Ethernet stack which can be used to implement the communication. Additional drivers will be implemented to support the custom-made interface devices of the HNS OBCs. The base software must also provide the support of time synchronization between the distributed subsystems. It is planned to use PTP [24], which provides a high accuracy and is an established standard protocol. RTEMS does not provide its own PTP implementation, but it is planned to port an existing library.

Furthermore, the base software contains a middleware placed between RTEMS plus drivers and the application. It serves as a hardware abstraction layer to access the interface devices like Ethernet and Universal Asynchronous Receiver/Transmitters (UART). The middleware also provides a runtime environment for the application. Hardware abstraction is done by using the DLR library called Open modular software Platform for Spacecraft (OUTPOST) [25]. It will be extended to support all interface devices.

To provide a runtime environment, the DLR Tasking Framework [26] will be used. It was developed to enable parallel computation of application on distributed on-board systems in a space environment. The application will be implemented in so-called tasks, which are scheduled and started by the Tasking Framework. Input data from interface devices are stored in so-called channels, which will trigger the tasks if a certain amount of data is stored. Using channels and tasks has the advantage that the application will run asynchronous to the input data from outside. This makes the application more resilient against deadlocks and input errors. The Tasking Framework was successfully used in previous projects like Autonomous Terrain-Based Optical Navigation (ATON) [27].

A specialty of the CALLISTO project is the usage of subsystems developed by CNES, DLR, and JAXA, which all interact with each other. Having said this, an agreed fundamental communication design between all three parties is required. Examples are the definition of a communication protocol on top of Ethernet and the already mentioned PTP. Verification of the software stack will be carried out finally using Hardware-in-the-Loop (HiL) simulation campaigns of the HNS together with the G&C parts.

4. Differential GNSS Approach

GNSS is a versatile measurement system that can support positioning applications with a wide range of performance requirements. While pseudorange-based standalone position measurements will generally be confined to a few meter accuracy, a centimeter-level accuracy can be achieved with geodetic-grade receivers and sophisticated carrier phase processing techniques (Figure 11). The latter include RTK [28] positioning with differential carrier phase observations of a reference station as well as Precise Point Positioning (PPP) [29] which requires provision of real-time GNSS orbit and clock corrections from a dedicated service provider. Both methods involve estimation and preferably fixing of carrier phase ambiguities which requires an appropriate initialization phase of varying duration before the desired performance can be achieved.

For CALLISTO, a 1 m (99-percentile) horizontal positioning accuracy is targeted during the final descent and landing phase. While this performance is well within the capabilities of currently available GNSS systems and correction services for common terrestrial users, CALLISTO poses specific challenges in terms of speed of motion, tracking conditions, and fast availability of navigation solutions after outages. Even though modern RTK engines making use of multi-GNSS observations can deliver a very rapid position fix for short baselines, it is difficult to anticipate that actual signal environment, measurement quality, and availability of differential measurements during the final descent. The use of carrier-phase-based RTK or PPP techniques is therefore deprecated in favor of purely pseudorange-based positioning that promises a higher robustness under the CALLISTO flight conditions as well as fully instantaneous solutions.

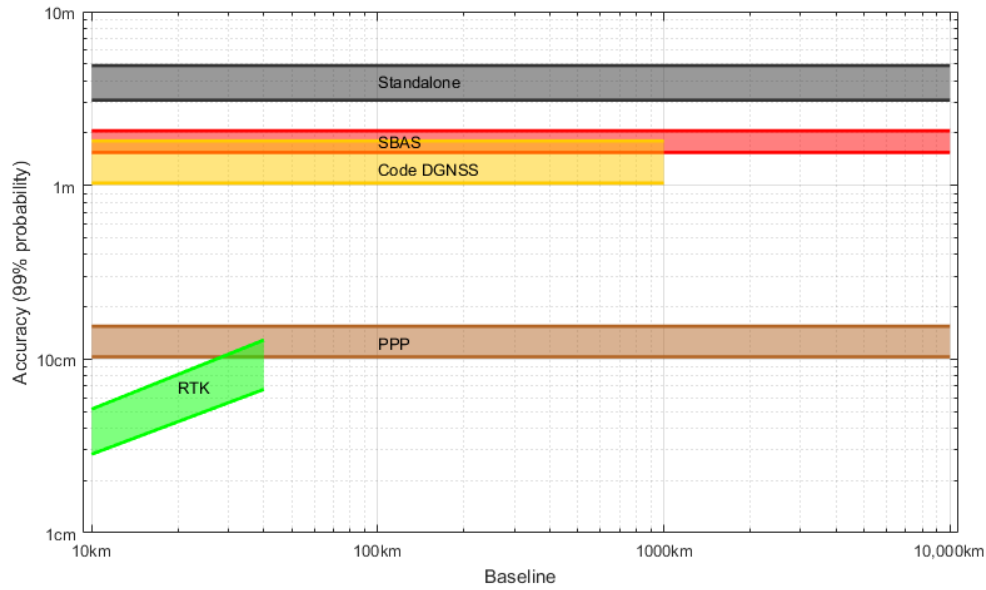


Figure 11: Rule of thumb accuracies of different GNSS positioning techniques. The upper line of each field represents the vertical accuracy, the lower line represents the horizontal accuracy. Assumes open sky conditions, geodetic-grade receivers, and antenna with proper multipath mitigation. (SBAS: Satellite-Based Augmentation System, DGNSS: Differential GNSS, PPP: Precise Point Positioning, RTK: Real-Time Kinematic).

A first assessment of the achievable navigation accuracy can be achieved by considering the Signal-in-Space Range Error (SISRE) of the tracked constellations, the typical User Equipment Errors (UEE) and the Dilution of Precision (DOP) [30]. For single-point positioning and considering only the horizontal component, the distance Root Mean Square (RMS) and the 99-percentile error (R_{99}) can be assessed using the relation

$$\text{DRMS} = \text{HDOP} \cdot \sigma_{\text{UERE}} = \text{HDOP} \cdot \sqrt{\sigma_{\text{SISRE}}^2 + \sigma_{\text{UEE}}^2} \quad (1)$$

$$R_{99} = 2.1460 \cdot \text{HDOP} \cdot \sqrt{\sigma_{\text{SISRE}}^2 + \sigma_{\text{UEE}}^2} \quad (2)$$

Following [31], GPS and Galileo presently achieve SISRE standard deviations of about 0.6 m and 0.2 m, respectively while receiver tracking errors (in a low multipath environment) amount to 0.9 m and 0.6 m for the envisaged receiver type. The latter can further be reduced to 0.6 m and 0.4 m when employing carrier phase smoothing with a 50 s averaging time scale. At representative Horizontal Dilution of Precision (HDOP) values of 1 for near equatorial locations, R_{99} values of about 1.5–2 m are achieved with the individual constellations using unsmoothed observations. These errors can further be reduced in a combined processing and by use of smoothed measurements. In fact, practical positioning tests conducted with a GNSS monitoring station at Kourou (KOUG) have demonstrated the feasibility of achieving an R_{99} horizontal positioning accuracy of about 1 m using either standalone Galileo or (more robustly) combined GPS+Galileo processing in a benign environment.

While this is marginally compliant with the needs of CALLISTO during the landing phase, additional performance can be gained by use of differential processing. For assessing the resulting relative positioning accuracy, Signal-in-Space (SIS) range errors in equations 1 and 2 can be replaced by the ranging errors of the reference station. Furthermore, ionospheric path delay differences over baselines of less than 1 km can safely be neglected, which enables use of single-frequency observations with a factor of three smaller noise level than the ionosphere-free combination of dual-frequency measurements. As a result, a better than 1 m R_{99} positioning error is achieved, which safely meets the specification. Furthermore, the DGNSS processing provides enhanced robustness and immunity against broadcast ephemeris errors that might impact a standalone positioning solution. It is therefore considered as baseline for the GNSS contribution to the HNS.

5. Navigation Performance Assessment

The performance of the HNS has been assessed by means of a covariance analysis for two reference trajectories, referred to as *Return-to-Launch-Site (RTLS)* and *Downrange (DR)*, which have been designed by JAXA and DLR to fit the Test and Demo Flight scenarios, respectively. Figure 12 shows a comparison between the downrange-altitude profiles of the two trajectories. For a matter of brevity, the navigation performance analysis results are shown here for the DR trajectory only, which was chosen because of the more challenging flight envelope, including larger velocity, acceleration, and attitude changes.

The time histories of some trajectory parameters are given in Figure 13 for the DR scenario. In the lower-right plot, showing the pitch rate profile, one can see the rotation maneuver that precedes the re-entry burn, visible in the specific acceleration plot (lower-left). The vertical grayed bands represent $\sim 10-15$ s intervals during which, in the failure case scenarios presented later in this section, it will be assumed that the GNSS signal is lost. These three intervals correspond approximately to the re-entry burn, to the maximum aerodynamic deceleration and to the last part of the landing burn.

An important assumption made for the ensuing analysis is that the GNSS receiver only provides the Single Point Positioning (SPP) solution, whereas the DGNSS solution is not available. This is because suitable performance figures for the latter are not yet available due to lack of heritage in the use of this technology for such kind of applications. Tests will be conducted to characterize the receiver's performance for a real-case scenario and the performance assessment will be updated once this data is available. For the time being, the SPP performance figures are used.

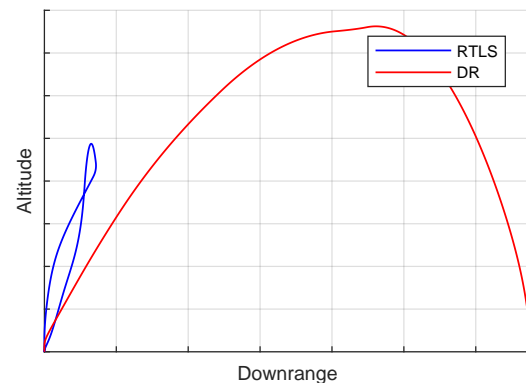


Figure 12: Downrange-altitude profiles comparison.

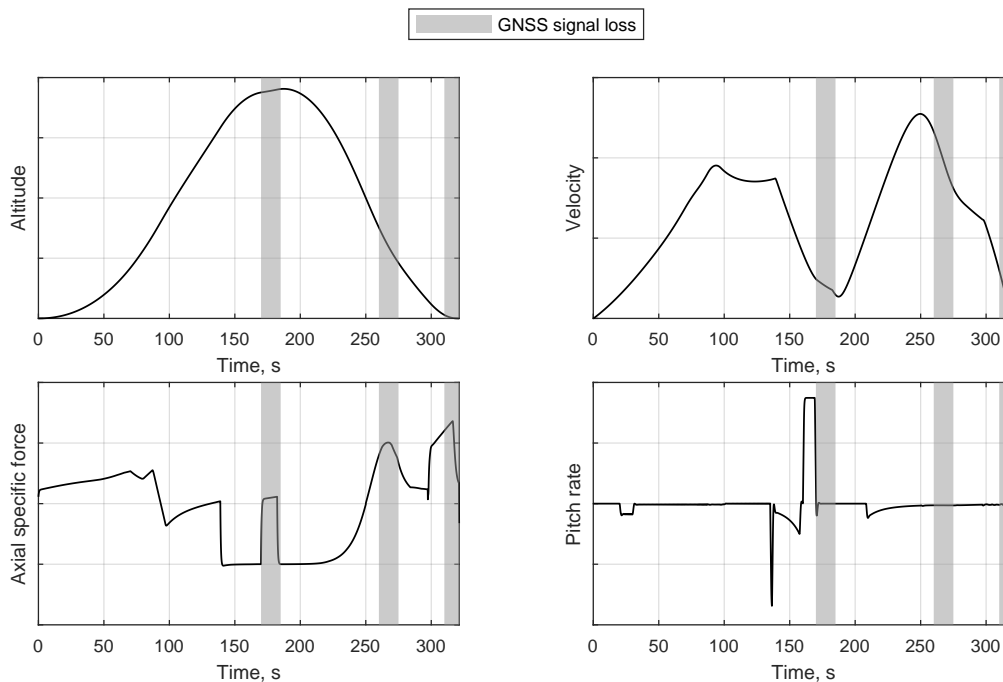


Figure 13: DR trajectory.

Nominal Scenario

In this section, the nominal scenario will be considered, which assumes the GNSS solution to be available throughout the entire trajectory and the radar altimeter to be operational below 500 m altitude, both with a measurement frequency of 10 Hz. Additional assumptions have been made regarding the configuration of the state estimator. The velocity error covariance has been initialized with a very small value, in light of the fact that the vehicle is stationary before launch and the only residual velocity, as coming from non-rigid structural effects, has zero-mean and can be accounted for as noise. This, together with knowledge of the local gravity vector, can be used for gyro compassing during the time preceding lift-off, improving the accuracy of the estimate of some IMU parameters, such as bias and scale factor, which are then further estimated during flight. For the sake of this analysis, at lift-off (i. e., at $t = 0$ s) the attitude error covariance is reset to a value close to zero. The results shown in the plots of Figure 14 should therefore be considered as the HNS “internal” performance, isolated from external mounting errors or vehicle structure misalignments with respect to the local vertical.

The time histories of the 1σ covariance bounds for position, velocity, and attitude error are reported in Figure 14 for the nominal scenario. In the top plot, one can see that the vertical position error is larger than the horizontal one during most of the flight, as is expected based on typical GNSS DOP values, but rapidly decreases towards the end of the flight as radar altimeter fixes become available. This does not show in the velocity plot, as the measurement error was assumed to be isotropic. Additionally, as external forces mainly act along the vehicle’s longitudinal axis, the components of the IMU parameters producing errors along this direction are better observable and, therefore, more accurately estimated. These factors lead to an overall better velocity estimate in the vertical direction. Finally, the bottom plot shows a rapid increase in attitude error around the roll axis during the ascent phase due to its limited observability. During the ballistic phase, the attitude change combined with the lack of observability produce further uncertainty growth, affecting most significantly the pitch and yaw components. Finally, during the re-entry burn, the presence of non-inertial accelerations in combination with the GNSS updates make attitude observable, thus causing the decrease in uncertainty visible in the plot.

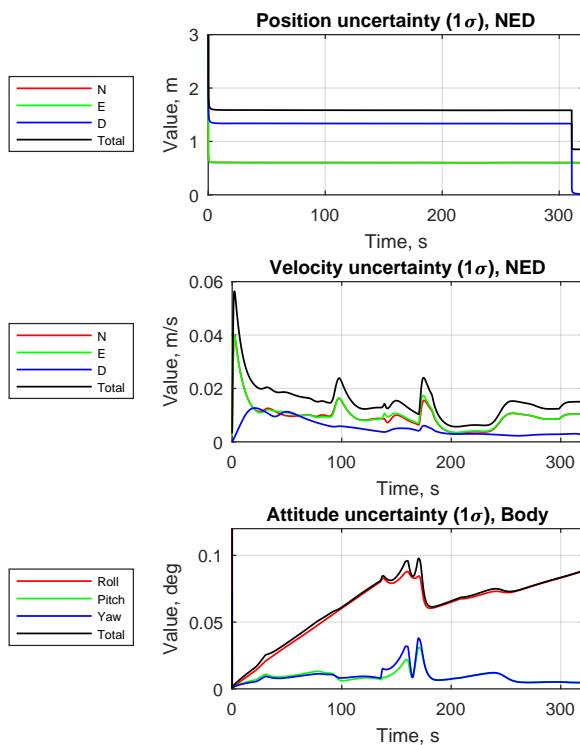


Figure 14: Nominal scenario.

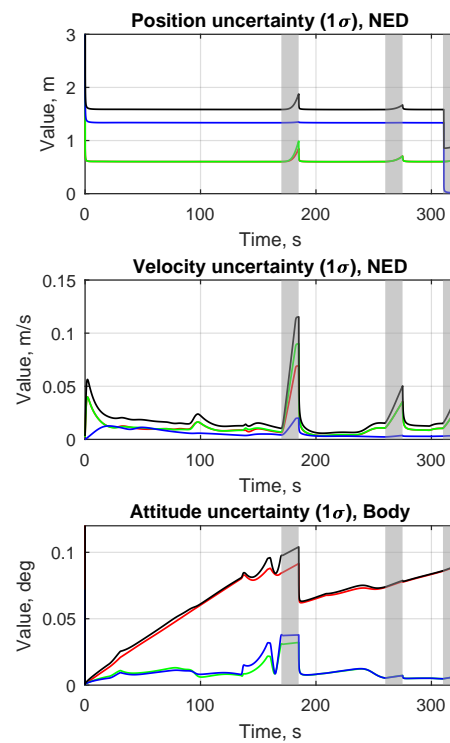


Figure 15: Failure Case 1: GNSS signal losses.

Failure Case Scenarios

As explained in Section 3.2, the radar altimeter was included to cope with specific requirements during the landing phase in terms of vertical position (0.5 m at 99 %, $\simeq 0.19$ m 1σ). On the other hand, the horizontal position requirement (1 m at 99 %, $\simeq 0.47$ m RMS) can only be addressed by making use of DGNSS, and can thus not be fully verified in the present analysis. Nevertheless, the robustness of the navigation system will be investigated with respect to GNSS signal losses. To this purpose, two failure cases are defined:

Failure Case 1: Three GNSS signal losses (as shown in Figures 13 and 15), of the duration of ~ 10 –15 s each, are assumed to occur at key moments during the mission, namely throughout the entire re-entry burn, during maximum aerodynamic deceleration and right before (and all the way to) touch-down. During these time intervals, the navigation system completely relies on inertial measurements, with the exception of radar altimeter measurements during the landing phase.

Failure Case 2: Neither GNSS nor radar altimeter fixes are available right before (and all the way to) touch-down. During this time interval, the navigation system completely relies on inertial measurements.

Figure 15 shows the time history of position, velocity, and attitude error covariance in presence of GNSS outages (the reader's attention is brought to the different y-axis scale for the velocity plot between Figures 14 and 15). One can see that, as attitude states are not directly observed by GNSS measurements, their estimation uncertainty is relatively little affected by the signal losses, even during the outage itself. On the other hand, position and velocity states, which are directly observed by GNSS measurements, are more significantly affected by signal losses. The outage producing the largest errors is the one occurring during the re-entry burn, as the IMU parameter uncertainties are larger at this point in time than they are further on along the trajectory. However, one can see that, so long as the GNSS solution becomes available again, the navigation system can quickly recover.

Finally, as the landing phase is an especially critical one, the last few hundreds of meters of descent are looked at in closer detail in the following. In doing so, the results obtained for Failure Case 2 (no GNSS + no radar altimeter) are compared with the nominal scenario. This comparison is shown in Figure 16. In this case, the focus is on vertical and horizontal position accuracy only, as velocity is well within the required value and attitude does not suffer significantly from such failures, as shown by Figure 15. One can see that, without radar altimeter updates, the vertical position estimate uncertainty would be above the required value at 100 m altitude. This is still expected to be the case if the DGNSS solution were available. For this reason, radar altimeter updates are considered critical to mission success. On the other hand, the horizontal position error is larger than the required value both in the nominal and in the failure case scenarios. However, as the currently achievable horizontal uncertainty is not as far from the required value as the vertical one is, the DGNSS corrections are expected to suffice in bridging this gap and bringing the horizontal position estimate uncertainty below the required value.

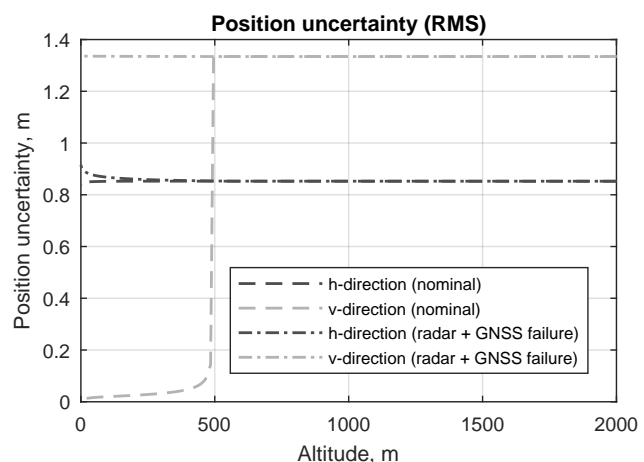


Figure 16: Failure Case 2: Radar altimeter and GNSS concurrent failures.

6. Conclusions and Outlook

Since the project is currently in Phase B, the design of the HNS is currently still at a very early stage. The requirements derived from the previous studies and set by the CALLISTO mission in terms of navigation turned out to be challenging. In order to satisfy these requirements, innovative approaches like the DGNSS concept and the radar altimeter system, which have not been applied to European launchers before, have been introduced into the HNS sensor suite. Preliminary performance analyses with the currently selected sensor suite have allowed verification of the compliance with most of the navigation performance requirements under nominal conditions, as well as for some failure scenarios.

Acknowledgements

The work described in this paper has been funded internally by the German Aerospace Center (DLR), Program Directorate Space Research and Technology, as part of the ongoing joint research activities of the French National Center for Space Studies (CNES), DLR, and the Japan Aerospace Exploration Agency (JAXA) in the frame of the trilateral project *Cooperative Action Leading to Launcher Innovation for Stage Tossback Operation (CALLISTO)*. The authors gratefully acknowledge the collaboration with CNES and JAXA and the valuable discussions with all members of the CALLISTO project team.

Abbreviations

AHRS	Attitude and Heading Reference System	IEEE	Institute of Electrical and Electronics Engineers
ALS	Approach and Landing System	ILS	Instrument Landing System
ATON	Autonomous Terrain-Based Optical Navigation	IMU	Inertial Measurement Unit
CAD	Computer-Aided Design	ITAR	International Traffic in Arms Regulations
CALLISTO	Cooperative Action Leading to Launcher Innovation for Stage Tossback Operation	JAXA	Japan Aerospace Exploration Agency <i>Japanese: 宇宙航空研究開発機構</i>
CNES	French National Center for Space Studies <i>French: Centre National d'Etudes Spatiales</i>	LH2	Liquid Hydrogen
COTS	Commercial Off-the-Shelf	LOx	Liquid Oxygen
CPU	Central Processing Unit	NDB	Non-Directional Beacon
CSG	Guiana Space Center <i>French: Centre Spatial Guyanais</i>	OBC	On-Board Computer
CVI	Immediate Visual Control <i>French: Contrôle Visuel Immédiat</i>	OBCDH	On-Board Computing and Data Handling
DAU	Data Acquisition Unit	OR	O-Ring
DC/DC	Direct Current-to-Direct Current	OUTPOST	Open modular software Platform for Spacecraft
DGNSS	Differential GNSS	PDOP	Position Dilution of Precision
DGS	DGNSS Subsystem	PDR	Preliminary Design Review
DLR	German Aerospace Center <i>German: Deutsches Zentrum für Luft- und Raumfahrt e. V.</i>	PDU	Power Distribution Unit
DME	Distance Measuring Equipment	PDU-C	PDU Controller
DOP	Dilution of Precision	PDU-M	PDU Monitor
DR	Downrange	PPP	Precise Point Positioning
EMC	Electromagnetic Compatibility	PPS	Pulse Per Second
EMI	Electromagnetic Interference	PR	Pseudorange
Eu:CROPIS	Euglena and Combined Regenerative Organic-Food Production in Space	PRR	Pseudorange Rate
FADS	Flush Air Data System	PTP	Precision Time Protocol
FCS/A	Flight Control System/Aerosurfaces	PVT	Position, Velocity, and Time
FCS/R	Flight Control System/Reaction Control System	QR	Quick Response
FCS/V	Flight Control System/Thrust Vectoring	ReFEX	Reusability Flight Experiment
FDIR	Failure Detection, Isolation, and Recovery	RLV	Reusable Launch Vehicle
FDR	Flight Data Recorder	RMS	Root Mean Square
FEE	Front-End Electronics	RTCM	Radio Technical Commission for Maritime Services
FoV	Field of View	RTEMS	Real-Time Operating System for Multiprocessor Systems
FPGA	Field-Programmable Gate Array	RTK	Real-Time Kinematic
G&C	Guidance and Control	RTLS	Return-to-Launch-Site
GNC	Guidance, Navigation and Control	SBAS	Satellite-Based Augmentation System
GNSS	Global Navigation Satellite System	SHEFEX II	SHarp Edge Flight EXperiment II
GPIO	General-Purpose Input/Output	SIS	Signal-in-Space
GPS	Global Positioning System	SISRE	Signal-in-Space Range Error
GSE	Ground Support Equipment	SOCQ	Safety and Operational Coordination Quarter
GSOC	German Space Operations Center	SPP	Single Point Positioning
HDOP	Horizontal Dilution of Precision	TC	Telecommand
HiL	Hardware-in-the-Loop	TM/TC	Telemetry and Telecommand
HNS	Hybrid Navigation System	ToF	Time of Flight
		UART	Universal Asynchronous Receiver/Transmitter
		UAS	Unmanned Aerial System
		UAV	Unmanned Aerial Vehicle
		UDP	User Datagram Protocol
		UEE	User Equipment Errors

HYBRID NAVIGATION SYSTEM (HNS) PRELIMINARY DESIGN FOR CALLISTO

VBS	Virtual Base Station	VTHL	Vertical Takeoff, Horizontal Landing
VEB	Vehicle Equipment Bay	VTVL	Vertical Takeoff, Vertical Landing
VHF	Very High Frequency	WAAS	Wide Area Augmentation System
VOR	VHF Omni-Directional Range		

References

- [1] Jean Desmariaux, Elisa Cliquet-Moreno, and Christophe Chavagnac. CALLISTO: its flight envelope and vehicle design. In *8th European Conference for Aeronautics and Space Sciences (EUCASS), Conference on "Reusable Systems for Space Access". July 1–4, 2019, Madrid, Spain*. EUCASS association, 2019.
- [2] Stephan Theil, Markus Schlotterer, Marcus Hallmann, Michael Conradt, Markus Markgraf, and Inge Vanschoenbeek. Hybrid Navigation System for the SHEFEX-2 Mission. In *AIAA Guidance, Navigation and Control Conference and Exhibit*, Honolulu, Hawaii, USA, August 18–21, 2008. AIAA Paper No. 2008-6991.
- [3] Stephan Theil, Markus Schlotterer, Michael Conradt, and Marcus Hallmann. Integrated Navigation System for the second SHarp Edge Flight EXperiment (SHEFEX-2). In *Proceedings of the 31th Annual AAS Guidance and Control Conference*, Breckenridge, Colorado, USA, February 1–6, 2008. AAS Paper No. 08-012.
- [4] Stephan Theil, Stephen Steffes, Malak Samaan, Michael Conradt, Markus Markgraf, and Inge Vanschoenbeek. Hybrid Navigation System for Spaceplanes, Launch and Re-Entry Vehicles. In *16th AIAA/DLR/DGLR International Space Planes and Hypersonic Systems and Technologies Conference*. AIAA, October 2009.
- [5] René Schwarz and Stephan Theil. A Fault-Tolerant On-Board Computing and Data Handling Architecture Incorporating a Concept for Failure Detection, Isolation, and Recovery for the SHEFEX III Navigation System. In *Proceedings of the 13th International Conference on Space Operations (SpaceOps), May 5–9, 2014, Pasadena, California*. American Institute of Aeronautics and Astronautics (AIAA), May 8, 2014. AIAA Paper No. 2014-1874.
- [6] Stephen Steffes, Stephan Theil, Malak A. Samaan, and Michael Conradt. Flight Results from the SHEFEX2 Hybrid Navigation System Experiment. In *2012 AIAA Guidance, Navigation, and Control Conference*, Minneapolis, Minnesota, USA, August 13–16, 2012. AIAA Paper No. 2012-4991.
- [7] Stephen Steffes. Real-Time Navigation Algorithm for the SHEFEX2 Hybrid Navigation System Experiment. In *2012 AIAA Guidance, Navigation, and Control Conference*, Minneapolis, Minnesota, USA, August 13–16, 2012. AIAA Paper No. 2012-4990.
- [8] Malak Samaan and Stephan Theil. Development of a Hybrid Navigation System for the Third Sharp Edge Flight Experiment (SHEFEX-3). In *2013 AAS/ALAA Astrodynamics Specialist Conference*, Hilton Head Island, South Carolina, USA, August 11–15, 2013. AAS Paper No. 13-877.
- [9] Stephen R. Steffes. *Development and Analysis of SHEFEX-2 Hybrid Navigation System Experiment*. PhD thesis, University of Bremen, April 2013.
- [10] Shinji Ishimoto, Pascal Tatioussian, and Etienne Dumont. Overview of the CALLISTO Project. In *32nd International Symposium on Space Technology and Science (ISTS). June 15–21, 2019, Fukui, Japan*, 2019.
- [11] Etienne Dumont, Shinji Ishimoto, Pascal Tatioussian, Josef Klevanski, Bodo Reimann, Tobias Ecker, Lars Witte, Johannes Riehm, Marco Sagliano, Sofia Giagkozoglou-Vincenzino, Ivaylo Petkov, Waldemar Rotärmel, René Schwarz, David Seelbinder, Markus Markgraf, Jan Sommer, Dennis Pfau, and Hauke Martens. CALLISTO: a Demonstrator for Reusable Launcher Key Technologies. In *32nd International Symposium on Space Technology and Science (ISTS). June 15–21, 2019, Fukui, Japan*, 2019.
- [12] Falcon 9 Launch Vehicle: Payload User’s Guide.
- [13] Patrick Rozas and Allen R. Cunningham. Apollo Experience Report: Lunar Module Landing Radar and Rendezvous Radar. Technical report, National Aeronautics and Space Administration (NASA), 1972. Report no. NASA TN D-6849.
- [14] André Hauschild, Markus Markgraf, Oliver Montenbruck, Horst Pfeuffer, Elie Dawidowicz, Badr Rmili, and Alain Conde Reis. Results of the GNSS receiver experiment OCAM-G on Ariane-5 flight VA 219. *Proceedings of the Institution of Mechanical Engineers Part G-Journal of Aerospace Engineering*, 231(6):1100–1114, 2016.
- [15] Waldemar Kunysz et al. High Performance GPS Pinwheel Antenna. In *Proceedings of the 2000 international technical meeting of the satellite division of the institute of navigation (ION GPS 2000)*, page 19–22, 2000.
- [16] Lars Johannsen. Erarbeitung eines Konzeptes zur aktiven Steuerung einer hochzuverlässigen Leistungsversorgungseinheit für ein hybrides Navigationssystem. Bachelor’s, Hochschule Bremen, July 2015.
- [17] Norbert Kwiatkowski. Entwicklung eines Referenzdesigns einer hochverfügbaren Leistungsversorgungseinheit für das Shefex III- Navigationssystem. Bachelor’s, Hochschule Wilhelmshaven, January 2014.
- [18] Norbert Kwiatkowski. Entwicklung von Test- und Verifikationsprozeduren für eine hochverfügbare Leistungsversorgungseinheit auf Basis einer Fehlermöglichkeits- und -einflussanalyse. Master’s thesis, Hochschule Wilhelmshaven, December 2015.

R. SCHWARZ, M. SOLARI, B. RAZGUS *et al.*

- [19] Samy Ayoub. Development of a Power Distribution Unit Controller for the SHEFEX III Navigation System. Master's thesis, Cologne University of Applied Sciences, July 2015.
- [20] Martin Reigenborn. Development and Verification of a Power Distribution Unit Controller Software for a Hybrid Navigation System. Master's thesis, Technische Universität Berlin, October 2018.
- [21] Real-Time Executive for Multiprocessor Systems. <http://www.rtems.org>. Accessed: 2019-06-11.
- [22] Alexander Krutwig AK and Sebastian Huber SH. RTEMS SMP Status Report. 2015.
- [23] Olaf Maibaum and Ansgar Heidecker. Software Evolution from TET-1 to Eu: CROPIS. In *10th IAA International Symposium on Small Satellites for Earth Observation*, 2015.
- [24] IEEE Standard for a Precision Clock Synchronization Protocol for Networked Measurement and Control Systems. <https://standards.ieee.org/standard/1588-2008.html>. Accessed: 2019-06-11.
- [25] OUTPOST - Open modular software Platform for Spacecraft. <http://github.com/DLR-RY/outpost-core>. Accessed: 2019-06-11.
- [26] Zain A. H. Hammadeh, Tobias Franz, Olaf Maibaum, Andreas Gerndt, and Daniel Lüdtkke. Event-Driven Multithreading Execution Platform for Real-Time On-Board Software Systems. In *Operating Systems Platforms for Embedded Real-Time applications (OSPRT)*, July 2019. to appear.
- [27] S. Theil, N. Ammann, F. Andert, T. Franz, H. Krüger, H. Lehner, M. Lingenauber, D. Lüdtkke, B. Maass, C. Paproth, and J. Wohlfeil. ATON (Autonomous Terrain-based Optical Navigation) for exploration missions: recent flight test results. *CEAS Space Journal*, 10(3):325–341, Sep 2018.
- [28] Dennis Odijk and Lambert Wanninger. "Differential positioning". In *Springer Handbook of Global Navigation Satellite Systems*, pages 753–780. Springer, 2017.
- [29] Jan Kouba, François Lahaye, and Pierre Tétreault. "Precise point positioning". In *Springer Handbook of Global Navigation Satellite Systems*, pages 723–751. Springer, 2017.
- [30] Richard B Langley, Peter JG Teunissen, and Oliver Montenbruck. "Introduction to GNSS". In *Springer Handbook of Global Navigation Satellite Systems*, pages 3–23. Springer, 2017.
- [31] Oliver Montenbruck, Peter Steigenberger, and André Hauschild. Multi-GNSS signal-in-space range error assessment—Methodology and results. *Advances in Space Research*, 61(12):3020–3038, 2018.